Cell and Molecular Biology Faculty Publications

Cell and Molecular Biology

4-9-2020

Stavudine exposure results in developmental abnormalities by causing DNA damage, inhibiting cell proliferation and inducing apoptosis in mouse embryos

Rui-Fang Ao

Yu-Xiang Liang

Xiao-Qing Liu

Kui Tan

Xiaoling Wang

See next page for additional authors

Authors

Rui-Fang Ao, Yu-Xiang Liang, Xiao-Qing Liu, Kui Tan, Xiaoling Wang, Dan Liu, Ting Zhang, Gongqin Sun, and Jun Xie

Stavudine exposure results in developmental abnormalities by causing DNA damage, inhibiting cell proliferation and inducing apoptosis in mouse embryos

Rui-Fang Ao[a],[1], Yu-Xiang Liang[a],[1], Xiao-Qing Liu[a], Kui Tan[a], Xiaoling Wang[a], Dan Liu[a], Ting Zhang[b],*, Gongqin Sun[c], Jun Xie[a],*

[a] Department of Biochemistry and Molecular Biology, Shanxi Key Laboratory of Birth Defect and Cell Regeneration, Shanxi Medical University, Taiyuan 030001, Shanxi, China
[b] Capital Institute of Pediatrics, Beijing 100020, China
[c] Department of Cell & Molecular Biology, University of Rhode Island, 389 CBLS Building, 120 Flagg Road, Kingston, RI, 02881, USA

ABSTRACT

Stavudine is an anti-AIDS drug widely used to prevent HIV transmission from pregnant mothers to the fetuses in underdeveloped countries for its low price. However, there is still a controversy on whether stavudine affects embryo development. In the current study, embryotoxicity of stavudine was evaluated using cultured mouse embryos with the concentrations: 5, 10, 15 μM and vehicle control. The data indicated that the effect of stavudine was dose-dependent at early neurogenesis. Stavudine exposure reduced somite numbers, yolk sac diameter, crown-rump length, and increased the rate of embryonic degeneration compared with the control. We chose the lowest but clearly toxic concentration: 5 μM to investigate the molecular mechanisms of the damage. At the molecular level, stavudine produced DNA damage, increased the levels of the phospho-CHK1 and cleaved-caspase-3, and decreased the expression level of proliferating cell nuclear antigen. These changes indicated that stavudine caused a coordinated DNA damage response, inhibited cell proliferation, and induced apoptosis in the embryos. Collectively these results suggest that stavudine exposure disturbs the embryonic development, and its use in pregnant mothers should be re-examined.

1. Introduction

Antiretroviral therapy during pregnancy has dramatically reduced the rate of mother-to-child transmission of HIV (Warszawski et al., 2008). However, the number of HIV-infected pregnant women has increased, which results in an increase in the number of babies who have been exposed in utero to antiretroviral therapy. Tenofovir is an effective nucleoside reverse transcriptase inhibitor with low toxicity (Easterbrook et al., 2014). It is widely used as an anti-HIV drug. However due to its relatively high cost, 3–7 million patients in South Africa are not receiving this treatment. Instead, it was proposed that stavudine be used as a low cost alternative (Persad and Emanuel, 2016). Consequently, stavudine-based anti-HIV therapy is widely used as a first line regimen in low- and middle-income countries (Venter et al., 2018). Yet, it remains uncertain whether stavudine exposure affects the growth and development of the embryo.

As a nucleoside reverse transcriptase inhibitor, stavudine has been used to treat HIV infection since 1994. It is generally recommended for prevention after a needle-stick injury or other potential exposures (Huang et al., 1992). Stavudine blocks HIV replication by undergoing intracellular phosphorylation and inhibiting HIV reverse transcriptase by causing DNA chain termination (Huang et al., 1992). Stavudine also appears to cause significant side effects, especially to embryo development. Toltzis et al. reported that stavudine induced embryotoxicity in the whole-embryo culture system in the blastocyst stage (Toltzis et al., 1994). Exposure to stavudine-based HIV therapy in the first trimester of pregnancy resulted in an increased rate of preterm birth, delayed language, and other developmental concerns (Van Dyke et al., 2016). Chappuy et al. observed that the concentrations of nucleoside analogue reverse transcriptase inhibitors were higher in the amniotic fluid than in maternal plasma (Chappuy et al., 2004). Thus there is a need to investigate whether the high amniotic fluid nucleoside analogue

---

* Corresponding authors.
  E-mail addresses: Zhangtingcv@126.com (T. Zhang), junxie@sxmu.edu.cn (J. Xie).
[1] These authors contributed equally to this work.

reverse transcriptase inhibitor concentrations have an effect on the development of fetus. Several other studies have also suggested that stavudine affects embryonic development, causing stillbirth, low birth weight (Bostan et al., 2010; Barreto et al., 2004), language problems (Divi et al., 2007) and neurodevelopmental defects (Stammberger et al., 1989). In contrast, other studies reported conflicting conclusions on the embryo toxicity of stavudine. Price et al. found that ddI/Stavudine combinations were not associated with developmental toxicity or adverse drug interactions in pregnant mice (CD1) (Price et al., 2006). The lack of developmental toxicity is confirmed by the results of Liu et al. (Liu et al., 2014) and Salminskaia et al. (Salminskaia, 2013).

The controversy may be more consequential considering that stavudine is a commonly substituted drug (35.5 %) in Africa and underdeveloped countries. While birth defects (Seidahmed et al., 2014) due to HIV drug use would bring a heavy burden to the families in any society (Luteijn et al., 2014), the effects would be even more devastating in economically and medically deprived societies. Thus, it is urgent to clarify the impact of stavudine on embryonic growth and development.

Embryotoxicity studies require a careful evaluation of the embryonic development and a precise estimation of the morphological differentiation of the embryo. Such studies often face two major problems. The first issue is how to remove maternal effects. It is sometimes difficult to distinguish the maternal effects from the drug effects on embryo development, as the maternal medical and metabolic conditions can sometimes be confused with the effects of drugs. The second issue is defining the stage of embryonic development. Each embryo may have its own temporal and spatial pattern of development. Meanwhile, there may be considerable individual variations in the reaction to stavudine. To overcome these issues, mouse embryos may be an appropriate model for studying embryotoxicity. Using whole embryo culture can remove the maternal effects and accurately define the embryonic developmental stage (Kulkeaw et al., 2009). The teratogenic effects on embryo growth and development can be accurately determined, with a well-defined scoring system for quantifying the development of morphological features. Whole embryo culture is visual (Pryor et al., 2012), easy to operate, and convenient for elucidating the mechanism of toxicity (Dunlevy et al., 2006).

In this study, we investigated the effects of stavudine on embryo growth and development using the whole embryo culture system. The results reveal that stavudine exposure results in extensive developmental abnormalities in mouse embryos by causing DNA damage, inhibiting embryonic cell proliferation and inducing cell apoptosis. This study provides further confirmation for the detrimental effects of stavudine on embryonic development and suggests a mechanism by which stavudine exerts such effects.

2. Materials and methods

2.1. Animal treatments

All procedures involving animal handling were approved by Animal Care and Use Committee of Shanxi Medical University. All of the experiments were carried out in accordance with the approved guidelines by Shanxi Medical University. C57BL/6 mice (11400500030643, 9–10 weeks, 18–23 g) were housed in specific pathogen-free (SPF) cages at an approved facility on a 12 h light/dark cycle and with controlled temperature (22℃) and humidity (40–60 %). Mouse embryos at GD8.5 (Causeret et al., 2016) were cultured under sterilized condition at 37℃ for 48 h in heat-inactivated rat serum (Tuntland et al., 1999). Stavudine was bought from MCE (Med Chem Express) and the catalogs number was # 3056-17-5. For the growth of embryos, we choose rat serum as the dissolvent to enhance the reliability of the experiments. Stavudine power was added to rat serum and completely dissolved at a final concentration of 1 mM for the stock solution, which was stored at -80 ℃. Working solution at concentration of 5, 10, and 15 μM were freshly

made from stock solution. At the end of culture, embryos were quantitatively assessed by the scoring system as Van Maele-Fabry described (Van Maele-Fabry et al., 1993). The yolk sac circulation, heart, caudal neural tube, fore-, mid-, hindbrain, otic system, optic system, branchial bars, forelimb, hindlimb and somites were separately scored. In addition, we measured and recorded yolk sac diameter, the crown-rump length, and the rate of degeneration of deformity. The control and stavudine-treated embryos were collected for subsequent experiments.

2.2. Hematoxylin and eosin (H&E) staining

Embryos were fixed in cold 4% formalin, dehydrated in gradient alcohol, cleared in xylene, embedded with paraffin, cut into 3 μm-thick sections, stained with hematoxylin and eosin (H&E) and observed under a light microscope.

2.3. TUNEL analysis

DNA breaks were evaluated by terminal deoxynucleotidyl transferase (TdT) dUTP nick-end labeling (TUNEL assay). Procedures were performed using the In Situ Cell Death Detection Kit (Roche, Mannheim, Germany). In brief, formalin-fixed and paraffin-embedded embryonic tissues of control and stavudine-treatment embryos were cut into 3-μm thick slices, which were incubated with terminal deoxynucleotidyl transferase and dUTP. 3, 3'-Diaminobenzidine was used for the color development. The TUNEL-positive cells were presented as dark brown and counted under light microscope in six equal-sized fields which were randomly chosen, and the data were presented as mean ± SD.

2.4. Proliferation and apoptosis analysis

Immunohistochemistry was performed as described previously (Liang et al., 2018). Cleaved caspase-3 and proliferating cell nuclear antigen (PCNA) were immunohistochemically stained in embryonic tissues. The slides were incubated with primary rabbit antibodies against cleaved caspase-3 (1:200, #9661, Cell Signaling Technology, USA), or PCNA (1:50, #92729, Abcam, UK), followed by goat anti-rabbit secondary biotinylated antibodies (Zhongshan Golden Bridge, Beijing, China). The positive signals were visualized by DAB (Zhongshan Golden Bridge, Beijing, China) under the microscope at 100 times magnification. We randomly chose three different visual areas within the same regions of each section and counted the positive cells.

2.5. Western blot analysis

Standard Western blotting (Liang et al., 2018) assay was used to analyze the levels of protein p-CHK1, cleaved caspase-3 and PCNA. Briefly, proteins (30 g) from each sample were fractionated by SDS-PAGE and transferred onto the PVDF membrane. The primary antibodies used in the immunoblot were anti-phospho-CHK1 (Ser345) (p-CHK1, 1:1000, #2341S, Cell Signaling Technology, USA), anti-cleaved caspase-3 (Asp175) (1:1000, #9661, Cell Signaling Technology, USA), anti-PCNA (EPR3822) (1:1000, #92729, Abcam, UK), anti-beta actin (1:1000, ZSGB-BIO, China), and anti-GAPDH (sc-25778, Santa Cruz Biotechnology, TX USA). Then the membrane was incubated in 5% nonfat milk containing HRP-conjugated secondary antibody (1:5000) for 1 h. Signals were detected by ECL Chemiluminescent kit (Millipore) and analyzed with image J software.

2.6. Statistical analysis

All quantitative data are expressed as mean ± SD. Statistical analyses were performed using SPSS13.0 (SPSS Inc., Chicago, IL, USA) software. We tested results by ANOVA for overall significance in parametric growth measurements: yolk sac diameter, crown and hip
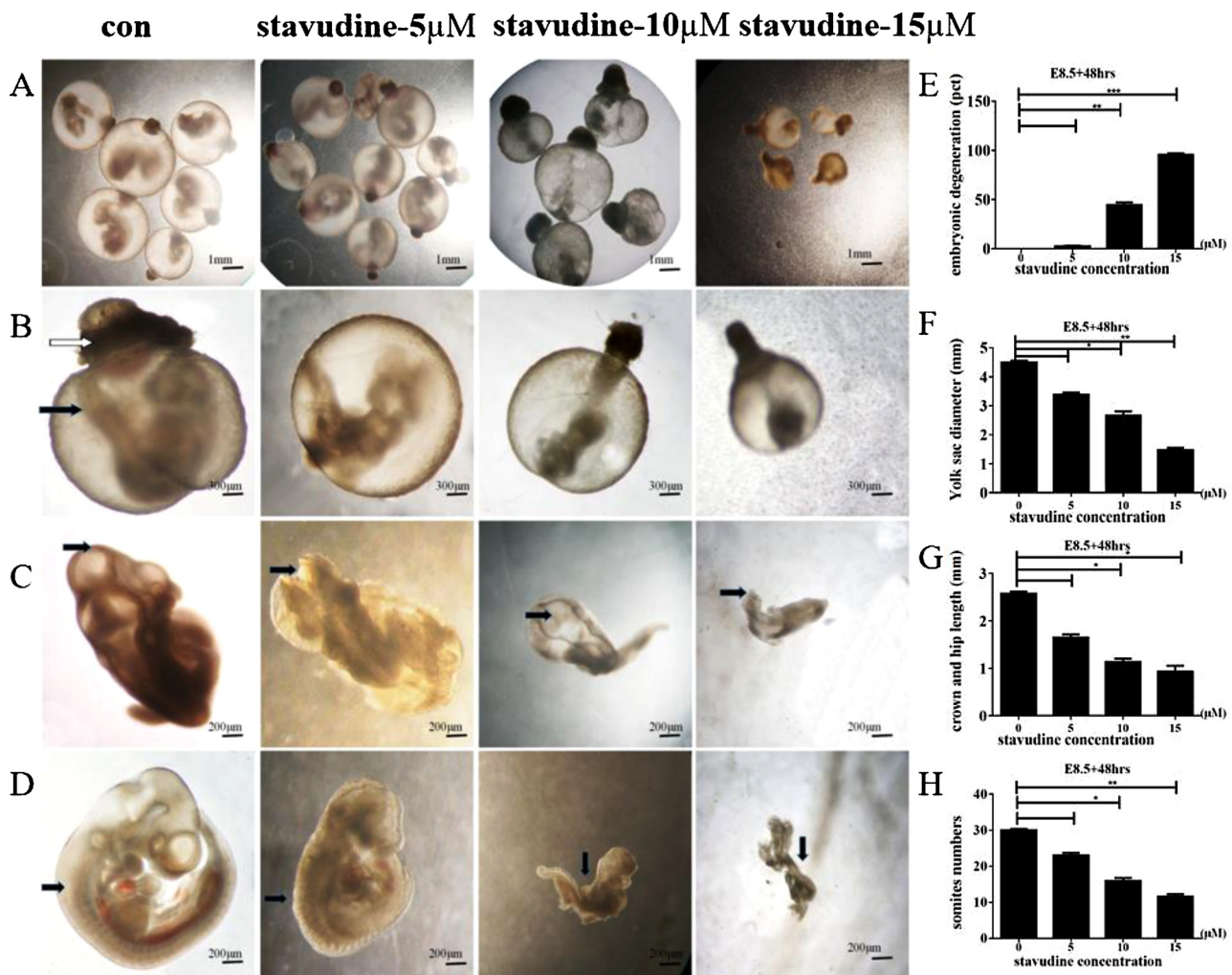
Fig. 1. Effect of stavudine-treatment on the morphology in embryos cultured for 48 h.
A-H showed embryos cultured in the presence of stavudine in concentrations of 0, 5, and 10 μM under dissecting microscope. A, images of the intact yolk sac in low magnification (scale bar ^{1} mm). B, embryos with the intact yolk sac in high magnificationyolk sac (white arrow) and ectoplacental cone (black arrow) (scale bar = 300 μm). C, yolk sac and ectoplacental cone were removed from embryos (scale bar = 200 μm). D, somites (short and black arrow) were decreased in a concentration-dependent manner (scale bar = 200 μm). E, F, G, and H quantification of the percentage of embryonic degeneration, Yolk sac diameter, crown-rump length and somites in embryos exposed to 0, 5, 10 and 15 μM Stavudine. E-H: The overall significance in parametric growth measurements was tested by ANOVA. Bonferroni method were adjusted for multiple comparisons of stavudine-treated serums versus control ***p ≤ .001, **p ≤ .01, *p ≤ .05; Student's t tests. n = 17.

length, embryo degeneration rate, and somite number, and Bonferroni method was adjusted for multiple comparisons of stavudine treated serums versus control.The data of PCNA, Tunel, CC3 and Western Blots were tested by *t*-test and P values less than or equal to 0.05 were significant.

3. Results

3.1. Morphological abnormalities in stavudine-treated embryos cultured for 48 h

To evaluate the effect of stavudine on embryonic development, E8.5 embryos were cultured for 48 h in the presence of 0, 5, 10, and 15 μM stavudine. We evaluated the potential detrimental effects of stavudine treatment on morphological and developmental parameters of murine embryos (Van Maele-Fabry et al., 1993) (Fig. 1). We observed general growth retardation in stavudine-treated embryos including retarded yolk sac diameter and reduced crown-rump length. The morphological and developmental parameters of embryos were assessed by a scoring system as previously described. The development of the control embryos was basically consistent with what Van Maele-Fabry described

(Van Maele-Fabry et al., 1993) (Fig. 1A-H). Significant differences in embryo morphology were observed between stavudine-treated groups and the control group (Fig. 1A-D). The number of somites, crown-rump length, and Yolk sac diameter between embryos exposed to 0, 5, 10, and 15 u M Stavudine decreased progressively with the increase in stavudine concentration, while the percentage of the embryo degeneration increased (Fig. 1E-H). Embryos treated with 5, 10, and 15 μM stavudine displayed lower total morphological scores compared with the control embryos (Figs. 1 and 2). In the 15 μM stavudine treatment, embryos displayed the lowest total morphological scores and many developmental parameters could not be detected, such as the hind-, mid-forebrain, otic vesicle, optic vesicle and so on.

The development of most organs was negatively affected by stavudine treatment in a concentration dependent manner. The results of dorsal-ventral flexure (embryo turning) showed a significant decrease in 5, 10 and 15 μM stavudine-treated embryos compared with the control embryos (Fig. 2). The control embryos completed turning, and appeared dorsally convex with spiral torsion, while embryos treated with 5 μM stavudine became C-shaped and appeared dorsally convex (Fig. 2). The embryos treated with 10 μM stavudine were still ventrally convex, and embryos treated with 15 μM stavudine almost fully
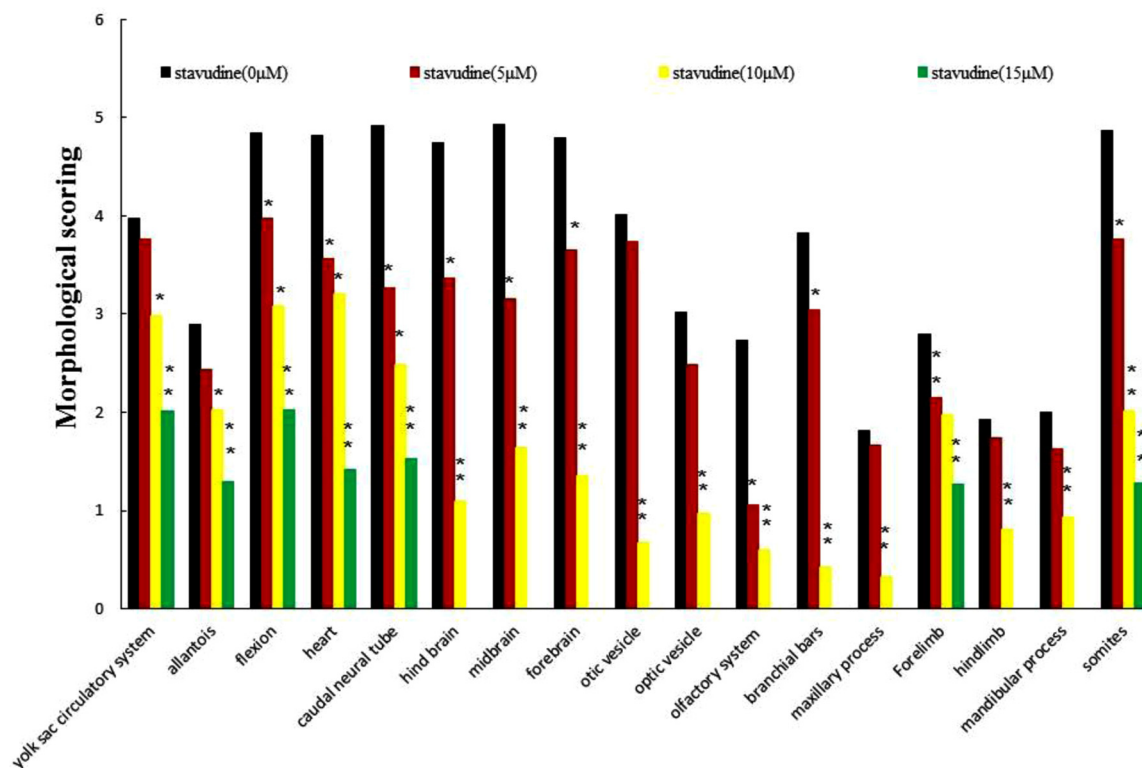
Fig. 2. Morphological scoring of embryos cultured for 48 h in stavudine-treatment by Van Maele-Fabry. Morphological scores of embryos treated with 0, 5, and 10 μM stavudine in the development of the brain, heart, neural tube, flexion, somites, and caudal neural tube. The 15 μM stavudine-treated embryos displayed the lowest total morphological scores and many developmental parameters could not be detected, such as the hind-, mid- forebrain, otic vesicle, optic vesicle and so on. The overall significance in parametric growth measurements was tested by ANOVA. Post hoc tests of stavudine-treated serums versus control. ***p ≤ .001, **p ≤ .01, *p ≤ .05; Student's t tests. n = 17.

undergone degeneration. Developmental abnormalities in the neural tube and the heart were also observed. Developmental parameters of the caudal neural tube decreased in the 5, 10 and 15 μM stavudine-treated embryos (Fig. 2) compared with the control embryos. A significant abnormalities of heart development was observed at 5 and 10 μM stavudine-treated embryos. The hearts in the 15 μM stavudine-treated embryos had no heart beat and stayed in 4–6 somites stage, while the normal embryos had 27–30 somites and four chambers. Heart appeared atrium commune and ventriculus communis in 5 μM stavudine-treated embryos. There was just a beating convoluted cardiac tube in 10 μM stavudine-treated embryos (Figs. 1 and 2).

The brain, including fore-, mid- and hindbrain, had also significant growth abnormalities in stavudine-treated embryos in a concentration-dependent manner compared to control embryos. The brain in the 15 μM stavudine-treated embryos stopped developing. In the hindbrain, the neural folds of the 10 μM stavudine-treated embryos also just had a V-shape in tangential view. The 5 μM stavudine-treated embryos had a partially fused rhombencephalon and a formed anterior neuropore with open folds, while the control groups had a completely closed anterior neuropore and a formed rhombencephalon with transparent roof of the 4th ventricle. In the middbrain, the neural folds of the 10 μM stavudine-treated embryos just had a V-shape in tangential view. The 5 stavudine-treated embryos had a partially fused mesencephalic folds (Fig. 1), while the control groups had a completely fused mesencephalon and a visible division between mesencephalon and diencephalon. In the forebrain, the 10 μM stavudine-treated embryos just had a V-shaped neural tube in tangential view. The 5 μM stavudine-treated embryos had partially fused prosencephalic folds while the control groups had completely fused and visible telencephalic evaginations (Fig. 2).

The four branchial bars are visible in the control embryos, while the

scores were lower in the 5 and 10 μM stavudine-treated embryos. The development of the mandibular, olfactory, and optic vesicle, otic vesicle in the 5 μM stavudine-treated embryos was similar to the control embryos, but significant developmental retardation was found in the 10 and 15 μM stavudine-treated embryos (P < 0.01). The result showed a significant degeneration rate (44.4 %) in the 15 μM stavudine treated-embryos, while the survived embryos displayed abnormal development and stunted organs (Fig. 2). We chose the lowest but clearly toxic concentration: 5 μM to investigate the molecular mechanisms of the damage.

3.2. Anatomical abnormalities in stavudine-treated embryos cultured for 48 h

In order to identify anatomical change, control and 5 μM stavudine-treated embryos were serially sectioned and subjected to histological analysis (n = 3). The development of the control embryos was similar to that described by Copp (Copp, 2005). There are significant differences in the brain tissue structure between the control and stavudine-treated embryos (Fig. 3A–G). The stavudine-treated embryos had relatively flat and narrow midbrain bubbles (Fig. 3B), smaller hindbrain vesicles, and more thinker roof plates of hindbrain (Fig. 3C). Neuroepithelial cells were loosened, and the wall of lumen was uneven, with some cells shrunken and detached in stavudine-treated embryos. We detected the first branchial arch, heart, somites, and tail in control embryos (Fig. 3D-G). In contrast, the stavudine-treated embryos lacked a thin and long tail compared with the control embryos (Fig. 3G).

3.3. TNEL in stavudine-treated embryos cultured for 48 h

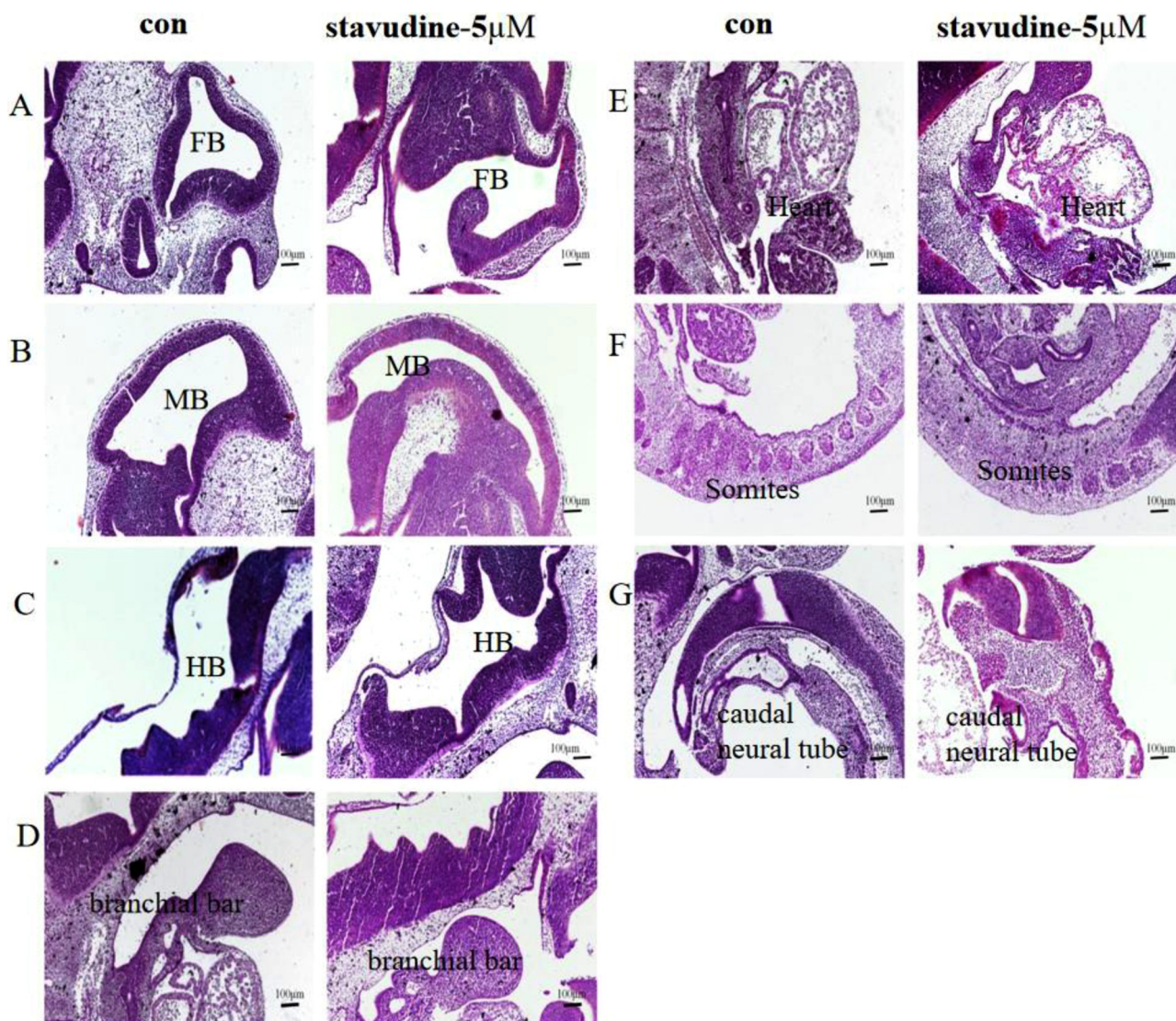Considering the significant developmental abnormalities in the

Fig. 3. Anatomical abnormalities of 5 μM stavudine-treated embryos cultured for 48 h. A-G showed structures of the forebrain, midbrain, hindbrain, heart, somites, branchial bars, and tail from normal embryos and 5 μM stavudine-treated embryos, n = 3, Scale bars indicated 100 μm.

stavudine-treated embryos, we assessed if the drug caused apoptosis by the terminal deoxynucleotidyl transferase (TdT) dUTP nick-end labeling (TUNEL) analysis. TUNEL-positive cells were significantly higher in stavudine-treated embryos than in the controls. In the controls, some TUNEL-positive cells were located in the fore and hindbrain. Increased amount of TUNEL-positive cells were seen throughout the fore and hindbrain in embryos exposed to 5 μM stavudine (Fig. 4A-C). We also found a significant increase in TUNEL positive cells in the 1 st branchial arch, the somites at the level of forelimb, and the tail in stavudine-treated embryos (Fig. 4D, F, G, andH $P < 0.05$), while a modest increase was seen in the midbrain compared with the controls and had no significant statistis (Fig. 4E, $P > 0.05$). These observations indicated that stavudine treatment caused significant and widespread apoptosis in the embryos (Fig. 4H, $P < 0.05$).

3.4. Effects on cell proliferation in stavudine treatment embryos cultured for 48 h

To explore the cellular basis of the developmental abnormalities, we investigated the effects of stavudine on cell proliferation in the embryos. Cell proliferation was assessed by determining the expression levels of proliferating cell nuclear antigen (PCNA) using

immunohistochemical staining. We found a large number of PCNA positive cells in the control embryos, but much reduced numbers in the 5 μM stavudine-treated embryos (Fig. 5A–G). The decrease of PCNA-positive cells in in fore-, midbrain, heart and caudal neural tube suggested that stavudine inhibited cell proliferation (Fig. 5H, $P < 0.05$).

3.5. Effects of stavudine treatment on cell apoptosis in embryos cultured for 48 h

To further determine if stavudine treatment induced apoptosis in mouse embryos, the immunohistochemically stained for the level of cleaved caspase-3 (Fig. 6A–G). Stavudine increased cleaved caspase-3 positive cells in the fore-, mid-, hindbrain, heart, somites and caudal tube (Fig. 6A-C, $P < 0.05$), heart, somites, and tail (Fig. 6E, F, G, H, $P < 0.05$), but did not significantly change the cleaved caspase-3 level in the 1 st branchial arch region (Fig. 6D, $P > 0.05$). The widespread increases in the cleaved caspase-3 levels suggested that 5 μM stavudine caused apoptosis in a large number of tissues (Fig. 6H, $P < 0.05$).
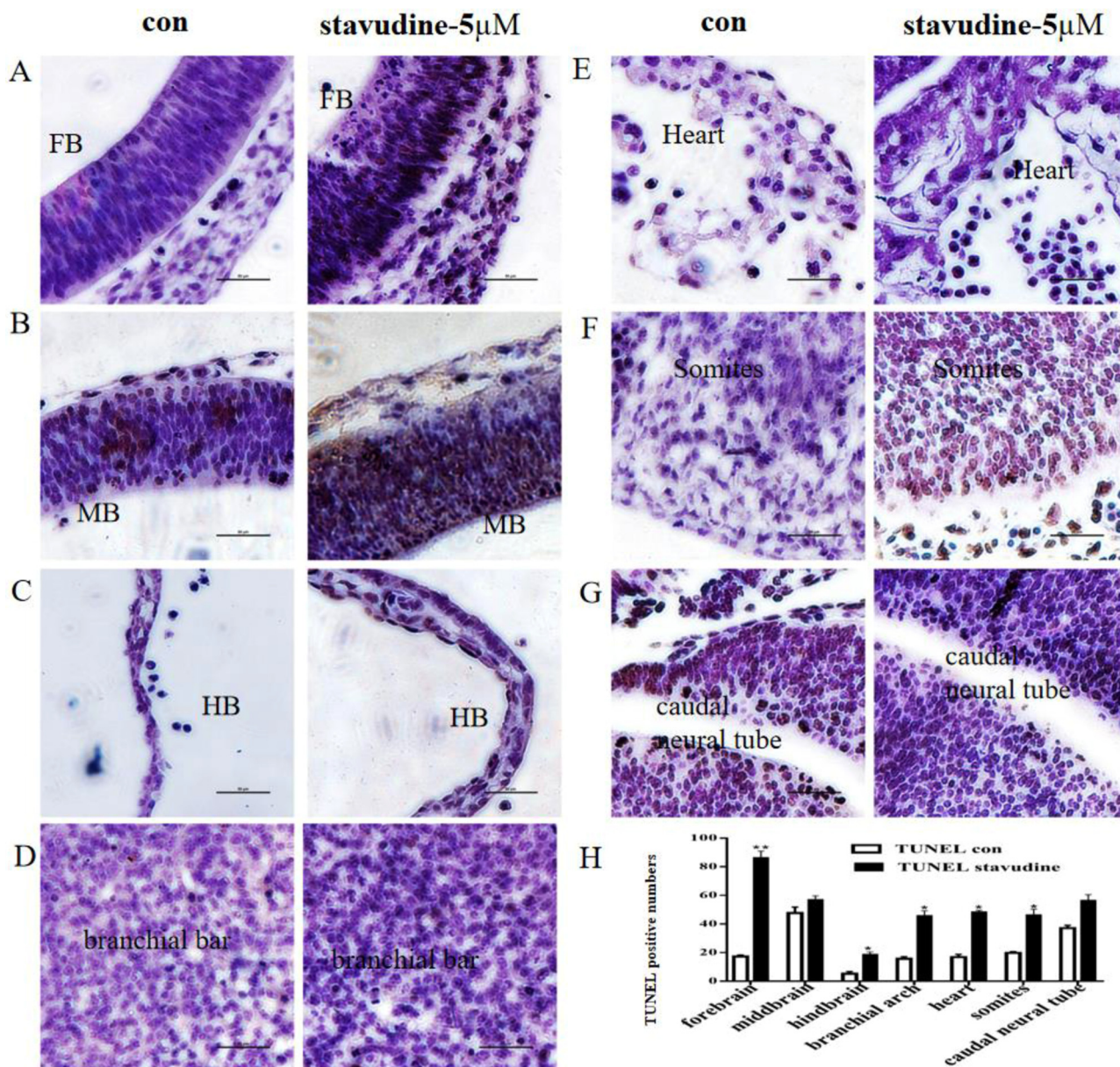
Fig. 4. Increased apoptosis in 5 μM stavudine-treated embryos cultured for 48 h. A-G, showed TUNEL results of forebrain, midbrain, hindbrain, heart, somites, branchial bars, and caudal neural tube in normal embryos (white bar) and 5 μM stavudine-treated embryos (black bar). Scale bar indicate 100 μm. H, quantification of the number of TUNEL positive cells 5 μM stavudine-treated embryos compared with controls. **p ≤ .01, *p ≤ .05; Student's t tests., n = 3.

3.6. Effects of stavudine on the levels of phospho-CHK1, cleaved caspased-3 and PCNA in embryos cultured for 48 h assessed by Western blot

To confirm the effects of 5 μM stavudine treatment on embryonic PCNA and cleaved caspase-3 levels observed in immunohistochemical staining, we further determined the expression levels of these and DNA damage response coordinating protein kinase CHK1 by Western blots (Fig. 7). Phospho-CHK1 (p-CHK1) is a critical protein kinase that gets activated by phosphorylation in response to DNA damage, which in turn coordinates DNA repair, cell cycle arrest and cell death. The results showed that the level of p-CHK1 in 5 μM stavudine-treated embryos was 2.37 times higher than in the control embryos (Fig. 7A-B, *P < 0.05). The protein level of cleaved caspase-3 in the 5 μM stavudine-treated embryos was 1.24 times higher than in the control embryos (Fig. 7C and D, *P < 0.05). Furthermore, the protein level of PCNA in the 5 μM stavudine-treated embryos decreased 22 % compared to the control embryos (Fig. 7E and F, *P < 0.05). These results

confirmed the immunohistochemical staining results, and further supported the conclusion that stavudine inhibited cell proliferation and induced the cell death, combined with DNA damage.

4. Discussion

The major goal of this study was to determine the effects of stavudine on the growth of embryo via the whole embryo culture platform. The parameters of growth and development decreased in many tissues and organs, including yolk sac diameter, somite numbers, turning, and branchial bars, while the rate of deformities and degeneration increased in the stavudine-treatment embryos. The study also provided new evidence that stavudine caused DNA damage, induced apoptosis of embryonic cells, and inhibited embryonic cell proliferation.

It is currently highly controversial if stavudine causes embryonic abnormalities. The range of human peak serum stavudine concentration is 3 − 10 μM when a patient is treated with clinically beneficial dose of
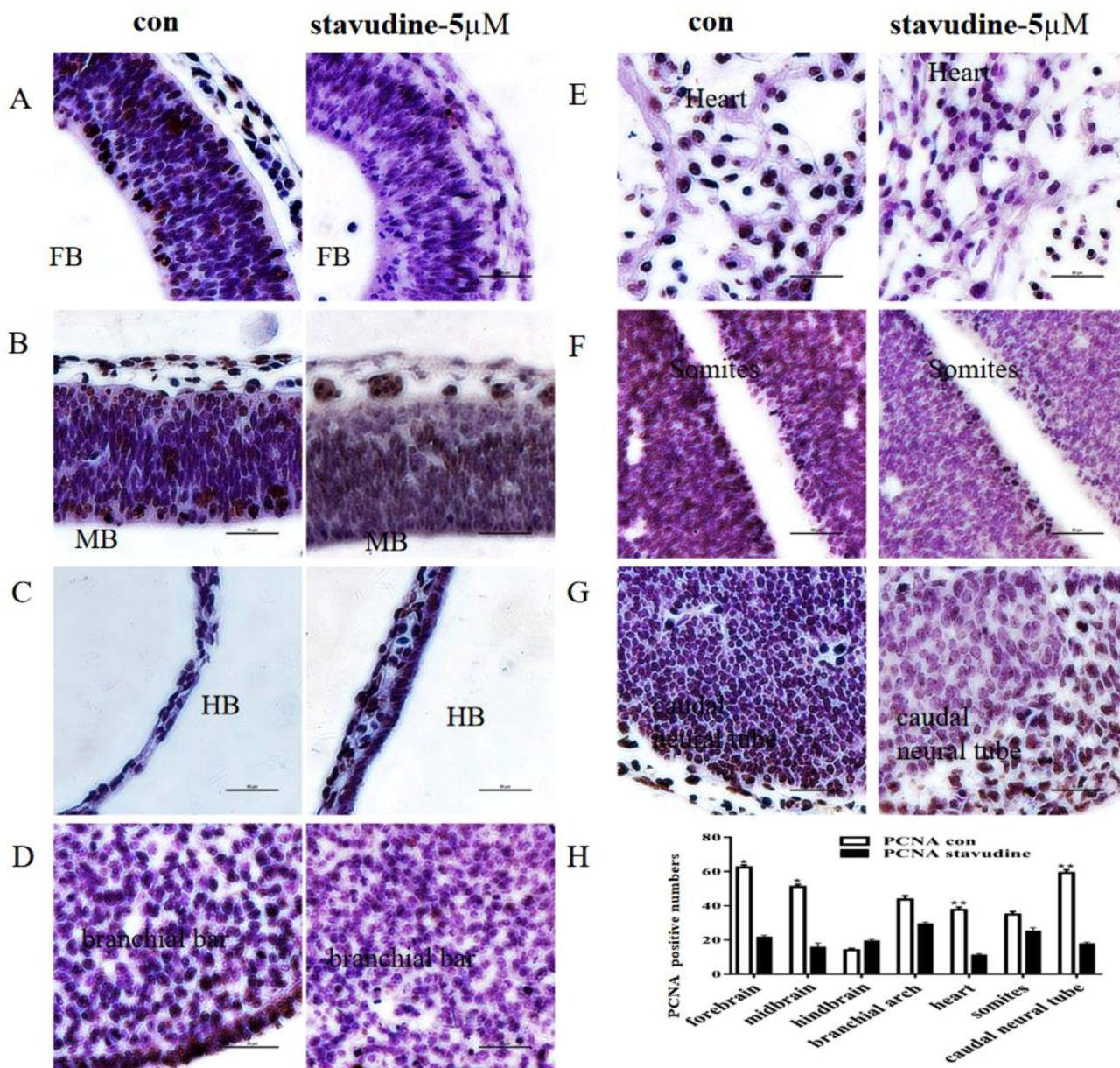
Fig. 5. Decreased proliferation in 5 μM stavudine-treated embryos cultured for 48 h. A-G, PCNA expression in the forebrain, midbrain, hindbrain, heart, somites, branchial bars, and caudal neural tube in normal (white bar) and stavudine-treated (5 μM) embryos (black bar). Scale bars indicate 100 μm. H, quantification of the number of PCNA positive cells in stavudine-treated and control embryos. **$p \leq$ .01, *$p \leq$ .05; Student's t tests., n = 3.

stavudine (Copp, 2005). The developmental anomalies induced by stavudine observed in the current study are caused by similar stavudine concentrations. The findings are consistent with the report by Toltzis and coworkers (Toltzis et al., 1994) suggesting that sublethal pre-blastocyst exposure to stavudine at 10 μM resulted in failure to develop beyond the blastocyst stage, even though we used post-implantation embryos, and they used pre-implantation embryos. The conclusion that stavudine damaged the development of embryos (Bostan et al., 2010; Barreto et al., 2004) is also supported by several other studies. However, Price et al. found that stavudine administered to pregnant CD1 mice by gavage had little effects on prenatal mortality, morphologic anomalies, and fetal body weight (Price et al., 2006). This result was confirmed by other similar studies by Liu et al. (2014) and Salminskaia (2013). The controversy may be due to the difficulty to compare results when the studies used different experimental set up (gavage feeding versus embryo culture) and the effect of assessment method. In the experiments with pregnant mice, it is not clear what concentration of

stavudine the embryos were exposed to, and what the maternal effects were on the study. The various effects of the drug on embryo development were also not directly measured. In contrast, the whole embryo culture platform we used in the current study provided a more direct and well controlled system for assessing the effects of stavudine on embryo development. Our results demonstrated that when embryos were directly exposed to stavudine, major developmental effects were observed. The system also allowed us to determine the mechanism by which stavudine exerted its effects: it caused extensive DNA damage, inhibited cell proliferation and induced apoptosis.

A key unknown in mouse experiments and in patients is the concentration of stavudine the embryos are exposed to. The range of human peak serum stavudine concentration is 3−10 μM when a patient is treated with clinically beneficial dose of stavudine (Horton et al., 1995). That is why we used the concentrations 5−15 μM in the current study. However, it is unknown what concentration of stavudine human embryos are actually exposed to in patients. A number of factors may
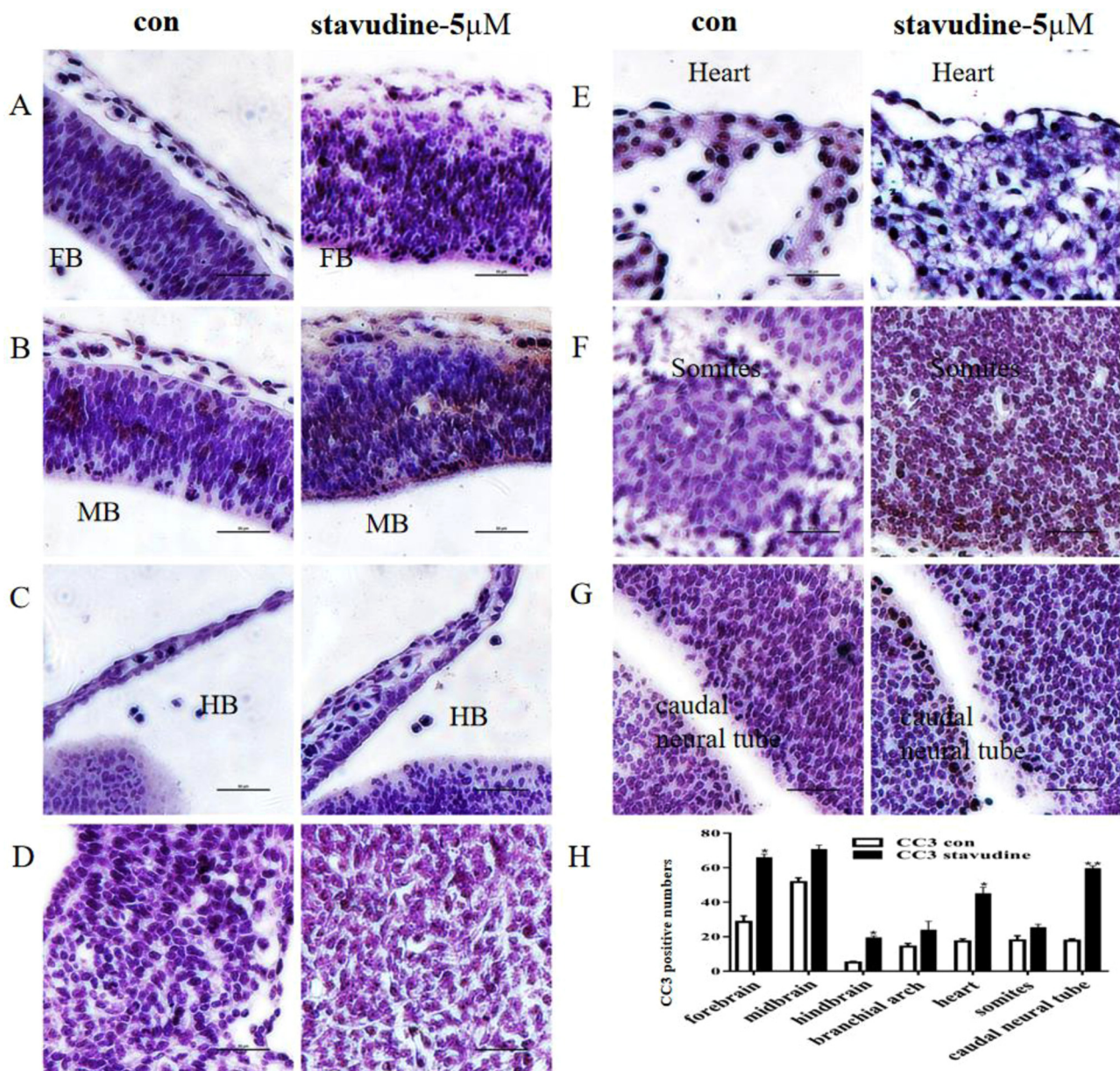
Fig. 6. Increased apoptosis in 5 μM stavudine-treated embryos cultured for 48 h. A–G, level of cleaved caspase-3 in forebrain, midbrain, hindbrain, heart, somites, branchial bars, and caudal neural tube in normal (white bar) and stavudine-treated embryos (black bar). Scale bars indicate 100 μm. H quantification of the number of cleaved caspase-3 positive cells in 5 μM stavudine-treated and control embryos. ***p ≤ .001 **p ≤ .01, *p ≤ .05; Student's t tests., n = 3.

affect the concentration of stavudine an embryo could be exposed to, and it is not well understood how the physiological changes of pregnancy may impact the antiretroviral pharmacokinetics. For example, Price et al. demonstrated that the stavudine internal concentration was lower in pregnant women than in other adults (Price et al., 2006), while Chappuy et al. (2004) indicated that stavudine is probably excreted through fetal urinary. In contrast, the urinary of whole embryo culture lacks the connection to the maternal system for excretion. Thus it is possible that the embryos are actually exposed to lower levels of stavudine, even though a patient have $3-10$ μM stavudine in the serum. It will be important to determine if there is a window of concentration of stavudine that can have the anti-viral benefits without causing developmental abnormalities. The concentrations we used are in the same ballpark as the concentration in the Chappuy study. With scarce pharmacokinetic information unavailable, our study is only mechanistic. Caution should be exercised in extrapolating such results directly and quantitatively into patients. With that said, the mechanistic insights

gained in this study will likely guide our understanding how HIV treatment may affect fetal development, at least qualitatively.

DNA instability during embryonic development would be expected to cause birth defect (Green et al., 2010). The results of p-chk1 analysis indicated that stavudine-treatment caused DNA damage in the embryos. DNA damage triggers DNA repair mechanisms. When DNA damage fails to be repaired, cell cycle will be stopped, and caspase-3 may be activated, which leads to apoptosis. Our findings suggested that the DNA damage response coordinating protein kinase CHK1 was activated, and active caspase-3 proteins was also markedly enhanced, and the number of PCNA positive cells decreased in neuroepithelial cells in the stavudine-treated embryos. These observations together would provide a mechanistic explanation for the stavudine embryonic toxicity. Although we have not yet investigated how stavudine causes DNA damage, it is plausible that as a nucleoside analog, stavudine may be recognized by some mouse or human DNA metabolic enzymes to interfere with DNA metabolism, resulting in DNA damage.
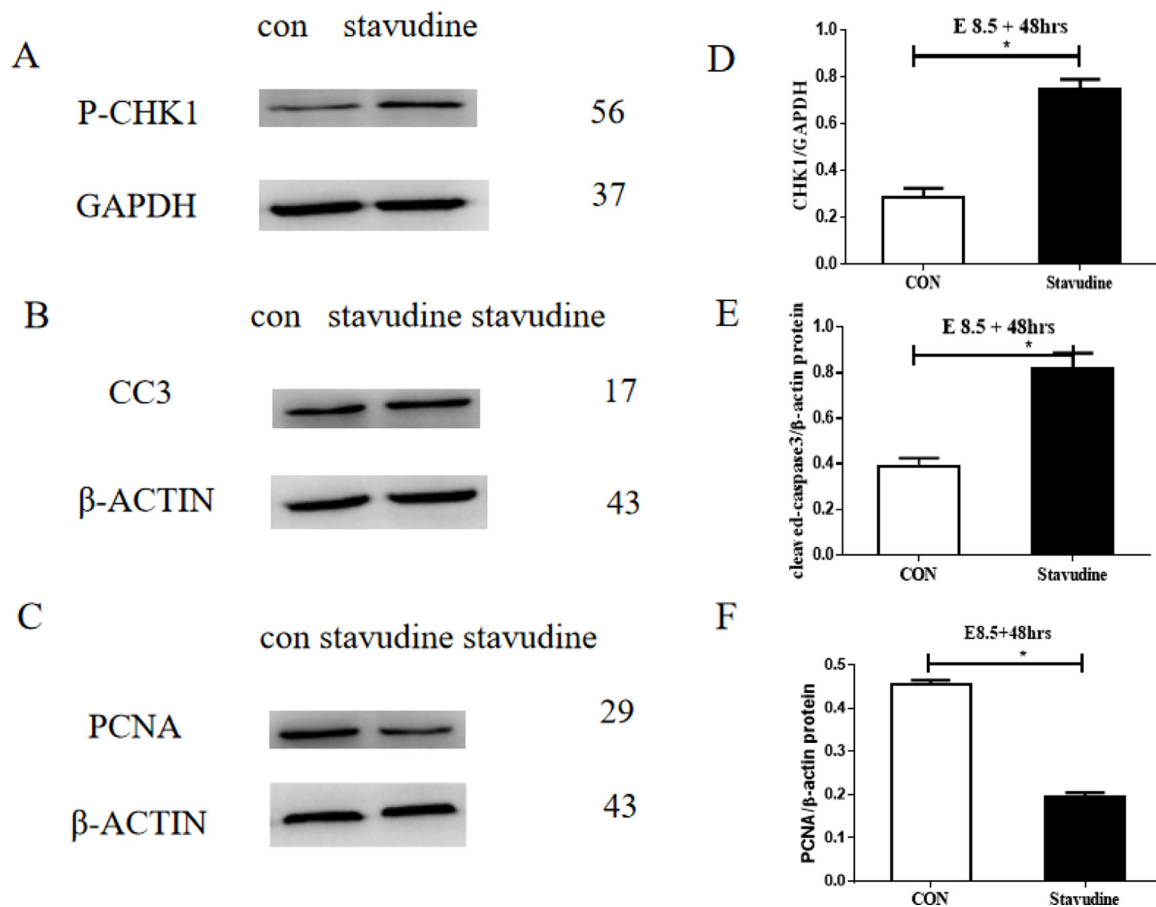
Fig. 7. Western blotting analysis of p-CHK1, cleaved caspase-3 and PCNA in embryos cultured for 48 h. A-F, Western blot and quantification of the protein p-CHK1, cleaved caspase-3 and PCNA. A, C, and E, representative Western blot results. B, D, and F, quantification of Western blot (SD are shown as error bars, N = 3. *P < 0.05). Black bar and white bar indicated control embryos and stavudine-treated (5 μM) embryos. *p ≤ .05; Student's t tests., n = 3.

Morphogenesis of the nervous system is based on a complex interplay among cell proliferation, differentiation and apoptosis (Greene and Copp, 2014). Increasing experimental evidence demonstrates that increased apoptosis and decreased proliferation caused by folate dysmetabolism are associated with neural tube abnormalities (Pai et al., 2015). Ke et al. concluded that apoptosis plays a crucial role in embryonic development, especially for midline fusion and aortic arch formation (Ke et al., 2018). Our results showed that DNA damage caused by stavudine, increased apoptosis and decreased proliferation in embryonic development. This imbalance is likely the underlying mechanism for the developmental abnormalities in stavudine-treated embryos.

In conclusion, it is well established that antiretroviral therapy can reduce the risk of passing the HIV infection from a mother to her child (Aaron and Cohan, 2013). However, possible adverse effects of anti-AIDS drugs on the development of the embryo are of great concern. Our study sheds light on the potential adverse effects and the mechanisms of such effects by stavudine. Perhaps the concentration of stavudine may be different in WEC and human fetal exposed. A key piece of information we lack is how much stavudine the embryo would be exposed to in a mother under HIV treatment. We wait with keen interest for such data that will provide critical guidance to future research on both stavudine toxicology and HIV treatment optimization.

Authors' contributions

RFA designed and performed experiments including major experiments and wrote the manuscript, YXL analyzed the data; XQL, Aaron and Cohan, 2013 KT, XLW, and DL performed minor experiments; GS designed the study, and wrote the manuscript. JX and TZ designed, supervised the study, and wrote the manuscript. All authors commented on the manuscript.

Declaration of Competing Interest

The authors declare that they have no known competing financial interests or personal relationships that could have appeared to influence the work reported in this paper. √

References

Aaron, E., Cohan, D., 2013. Preexposure prophylaxis for the prevention of HIV transmission to women. AIDS (London, England) 27, F1–5.
Barreto, R.L., de Jesus Simões, M., Amed, A.M., Soares Júnior, J.M., Oliveira-Filho, R.M., Kulay, L., 2004. Stavudine effects on rat pregnancy outcome. J. Obstet. Gynaecol. Res. 30, 242–245.

Bostan, A., Demeestere, I., Vanderwinden, J.M., Devreker, F., Englert, Y., 2010. Nucleoside analog stavudine depletes mitochondrial DNA with no organelle loss in mouse oocytes. Curr. HIV Res. 8, 127–133.

Causeret, F., Sumia, I., Pierani, A., 2016. Kremen1 and Dickkopf1 control cell survival in a Wnt-independent manner. Cell Death Differ. 23, 323–332.

Chappuy, H., Tréluyer, J.M., Jullien, V., Dimet, J., Rey, E., Fouché, M., Firtion, G., Pons, G., Mandelbrot, L., 2004. Maternal-fetal transfer and amniotic fluid accumulation of nucleoside analogue reverse transcriptase inhibitors in human immunodeficiency virus-infected pregnant women. Antimicrob. Agents Chemother. 48, 4332–4336.

Copp, A.J., 2005. Neurulation in the cranial region–normal and abnormal. J. Anat. 207, 623–635.

Divi, R.L., Leonard, S.L., Kuo, M.M., Nagashima, K., Thamire, C., St Claire, M.C., Wade, N.A., Walker, V.E., Poirier, M.C., 2007. Transplacentally exposed human and monkey newborn infants show similar evidence of nucleoside reverse transcriptase inhibitor-induced mitochondrial toxicity. Environ. Mol. Mutagen. 48, 201–209.

Dunlevy, L.P., Burren, K.A., Chitty, L.S., Copp, A.J., Greene, N.D., 2006. Excess methionine suppresses the methylation cycle and inhibits neural tube closure in mouse embryos. FEBS Lett. 580, 2803–2807.

Easterbrook, P.J., Doherty, M.C., Perriëns, J.H., Barcarolo, J.L., Hirnschall, G.O., 2014. The role of mathematical modelling in the development of recommendations in the 2013 WHO consolidated antiretroviral therapy guidelines. AIDS (London, England) S85–92.

Green, R.F., Devine, O., Crider, K.S., Olney, R.S., Archer, N., Olshan, A.F., Shapira, S.K., 2010. Association of paternal age and risk for major congenital anomalies from the National Birth Defects Prevention Study, 1997 to 2004. Ann. Epidemiol. 20, 241–249.

Greene, N.D., Copp, A.J., 2014. Neural tube defects. Annu. Rev. Neurosci. 37, 221–242.

Horton, C.M., Dudley, M.N., Kaul, S., Mayer, K.H., Squires, K., Dunkle, L., Anderson, R., 1995. Population pharmacokinetics of stavudine (d4T) in patients with AIDS or advanced AIDS-related complex. Antimicrob. Agents Chemother. 39, 2309–2315.

Huang, P., Farquhar, D., Plunkett, W., 1992. Selective action of 2',3'-didehydro-2',3'-di-deoxythymidine triphosphate on human immunodeficiency virus reverse transcriptase and human DNA polymerases. J. Biol. Chem. 267, 2817–2822.

Ke, F.F.S., Vanyai, H.K., Cowan, A.D., Delbridge, A.R.D., Whitehead, L., Grabow, S., Czabotar, P.E., Voss, A.K., Strasser, A., 2018. Embryogenesis and adult life in the absence of intrinsic apoptosis effectors BAX, BAK, and BOK. Cell 173, 1217–1230 e1217.

Kulkeaw, K., Mizuochi, C., Horio, Y., Osumi, N., Tsuji, K., Sugiyama, D., 2009. Application of whole mouse embryo culture system on stem cell research. Stem Cell Rev. Reports 5, 175–180.

Liang, Y.X., Liu, L., Jin, Z.Y., XH Liang, Y.S.Fu, Gu, X.W., Yang, Z.M., 2018. The high concentration of progesterone is harmful for endometrial receptivity and decidualization. Sci. Rep. 8, 712.

Liu, K.C., Farahani, M., Mashamba, T., Mawela, M., Joseph, J., Van Schaik, N., Honey, E., Gill, M., Jassat, W., Stringer, E.M., Chintu, N., Marlink, R.G., 2014. Pregnancy outcomes and birth defects from an antiretroviral drug safety study of women in South Africa and Zambia. AIDS (London, England) 28, 2259–2268.

Luteijn, J.M., Dolk, H., Addor, M.C., Arriola, L., Barisic, I., Bianchi, F., Calzolari, E.,

Draper, E., Garne, E., Gatt, M., Haeusler, M., Khoshnood, B., McDonnell, B., Nelen, V., O'Mahony, M., Mullaney, C., Queisser-Luft, A., Rankin, J., Tucker, D., Verellen-Dumoulin, C., de Walle, H., Yevtushok, L., 2014. Seasonality of congenital anomalies in Europe. Birth Defects Res. Part A Clin. Mol. Teratol. 100, 260–269.

Pai, Y.J., Leung, K.Y., Savery, D., Hutchin, T., Prunty, H., Heales, S., Brosnan, M.E., Brosnan, J.T., Copp, A.J., Greene, N.D., 2015. Glycine decarboxylase deficiency causes neural tube defects and features of non-ketotic hyperglycinemia in mice. Nat. Commun. 6, 6388.

Persad, G.C., Emanuel, E.J., 2016. The ethics of expanding access to cheaper, less effective treatments. Lancet (London, England) 388, 932–934.

Price, C.J., George, J.D., Marr, M.C., Myers, C.B., Bieler, G.S., Williams, R.L., Jahnke, G.D., 2006. Prenatal developmental toxicity evaluation of 2',3'-dideoxyinosine (ddI) and 2',3'-didehydro-3'-deoxythymidine (d4T) co-administered to Swiss Albino (CD-1) mice. Birth Defects Res. B Dev. Reprod. Toxicol. 77, 207–215.

Pryor, S.E., Massa, V., Savery, D., Greene, N.D., Copp, A.J., 2012. Convergent extension analysis in mouse whole embryo culture. Methods Mol. Biol. (Clifton, N.J.) 839, 133–146.

Salminskaia, O.I., 2013. [Experience with Invirase as part of triple therapy as the drug of choice in the perinatal prevention of HIV transmission in the Ul'ianovsk Region]. Terapevticheskii arkhiv 85, 16–20.

Seidahmed, M.Z., Abdelbasit, O.B., Shaheed, M.M., Alhussein, K.A., Miqdad, A.M., Khalil, M.I., Al-Enazy, N.M., Salih, M.A., 2014. Epidemiology of neural tube defects. Saudi Med. J. S29–35.

Stammberger, I., Schmahl, W., Tempel, K., 1989. Scheduled and unscheduled DNA synthesis in chick embryo liver following X-irradiation and treatment with DNA repair inhibitors in vivo. Int. J. Radiat. Biol. 56, 325–333.

Toltzis, P., Mourton, T., Magnuson, T., 1994. Comparative embryonic cytotoxicity of antiretroviral nucleosides. J. Infect. Dis. 169, 1100–1102.

Tuntland, T., Odinecs, A., Pereira, C.M., Nosbisch, C., Unadkat, J.D., 1999. In vitro models to predict the in vivo mechanism, rate, and extent of placental transfer of dideoxynucleoside drugs against human immunodeficiency virus. Am. J. Obstet. Gynecol. 180, 198–206.

Van Dyke, R.B., Chadwick, E.G., Hazra, R., Williams, P.L., Seage, G.R., 2016. The PHACS SMARTT study: assessment of the safety of in utero exposure to antiretroviral drugs. Front. Immunol. 7, 199.

Van Maele-Fabry, G., Delhaise, F., Gofflot, F., Picard, J.J., 1993. Developmental table of the early mouse post-implantation embryo. Toxicol. In Vitro 7, 719–725.

Venter, W.D.F., Kambugu, A., Chersich, M.F., Becker, S., Hill, A., Arulappan, N., Moorhouse, M., Majam, M., Akpomiemie, G., Sokhela, S., Poongulali, S., Feldman, C., Duncombe, C., Brown Ripin, D.H., Kumarasamy, N., 2018. Efficacy and safety of tenofovir disoproxil fumarate versus low-dose stavudine over 96 weeks: a multi-country randomised, non-inferiority trial. J. Acquir. Immune Defic. Syndr.

Warszawski, J., Tubiana, R., Le Chenadec, J., Blanche, S., Teglas, J.P., Dollfus, C., Faye, A., Burgard, M., Rouzioux, C., Mandelbrot, L., 2008. Mother-to-child HIV transmission despite antiretroviral therapy in the ANRS French Perinatal Cohort. AIDS (London, England) 22, 289–299.